



High B_s of FePBCCu nanocrystalline alloys with excellent soft-magnetic properties

Long Hou^a, Weiming Yang^{b,*}, Qiang Luo^a, Xingdu Fan^a, Haishun Liu^b, Baolong Shen^{a,b,*}

^a Jiangsu Key Laboratory for Advanced Metallic Materials, School of Materials Science and Engineering, Southeast University, Nanjing 211189, China

^b Institute of Massive Amorphous Metal Science, China University of Mining and Technology, Xuzhou 221116, China



ARTICLE INFO

Keywords:

Amorphous/nanocrystalline alloy
Soft-magnetic properties
Microstructure
 α -Fe nanocrystal

ABSTRACT

High saturation magnetic flux density (B_s) nanocrystalline alloys are increasingly attractive due to their unique microstructure and outstanding magnetic performance. In this work, we report that the substitution of B for P essentially improves the B_s of FePBCCu amorphous alloys. Based on high B_s amorphous matrix, the $\text{Fe}_{83.2}\text{P}_8\text{B}_2\text{C}_6\text{Cu}_{0.8}$ nanocrystalline alloy with high B_s of 1.77 T, low coercivity of 3.6 A/m and high effective permeability of 20,600 was developed. Such magnetic performance of $\text{Fe}_{83.2}\text{P}_8\text{B}_2\text{C}_6\text{Cu}_{0.8}$ nanocrystalline alloy is closely associated with the uniform refined composite microstructure, where the α -Fe nanocrystals with high volume fraction, small size and high number density ($\sim 1.8 \times 10^{23} \text{ m}^{-3}$) were formed. This finding makes the FePBCCu composite a kind of promising soft-magnetic material in electrical and electronic fields.

1. Introduction

As key functional materials, Fe-based nanocrystalline alloys (NAs) have promoted the development of electronic products toward high efficiency, energy saving, miniaturization and lightweight in modern electronic industry due to the high saturation magnetic flux density (B_s), low coercivity (H_c), high effective permeability (μ_e) and low loss (P) [1,2]. In developing Fe-based NAs, the excellent soft-magnetic properties (SMPs) and high B_s are mostly of interest from a scientific and applied point of view. Recently, a series of novel Fe-based NAs such as FeSiBNbCu [3], FeNiB(Si) [4,5], FeBSi(C)PCu [6,7], FeBSiCu [8,9] and FePCCu [10,11] alloy systems were successfully developed. Among these alloys, FePCCu nanocrystalline system shows low coercivity, high permeability, as well as low core loss [10], which is expected to make all kinds of magnetic devices, such as choke coils, power transformers and magnetic sensors, etc. However, compared to silicon steels with high magnetic flux density of ~ 2.0 T, this Fe-based NA shows low B_s of 1.65 T normally, seriously restricting its large-scale application as high magnetic flux component. Generally speaking, the higher Fe content is, the much higher B_s can be obtained, whereas the high Fe content of ~ 85 at.% is close to the upper limit of a single amorphous formation [12,13], which largely affects the multiple magnetic performance of Fe-based NAs designed in the later stage due to the coarse α -Fe grains embedded in amorphous matrix. Thus, how to balance this amorphous formability and magnetic performance of Fe-based NAs is a key

problem to be solved urgently. It was found that the B_s can be promoted by enhancing the exchange-coupling interaction of magnetic atoms [14,15]. As we known, the atomic radius of P (0.109 nm) is much larger than one of B (0.09 nm) [16]. Partial substitution of B for P means the increment of nearest-neighbor Fe atoms in FePCCu system. Therefore, improved B_s can be expected in the B-modified FePCCu NAs. Meanwhile, the previous work has pointed out that proper B addition into the FePC amorphous alloys can enhance the amorphous forming ability (AFA), even refine the microstructure, promoting the excellent magnetic performance [17]. All these analyses inspire us to explore the magnetic performance of FePCCu alloy system with partial substitution of B for P.

In this work, the FePBCCu amorphous alloys with good amorphous formability, high thermal stability and enhanced B_s were successfully synthesized. Based on high B_s amorphous matrix, the FePBCCu NAs with excellent SMPs were also developed. The amorphous formability, thermal stability and microstructure related to magnetic performance of FePBCCu alloys were investigated in detail.

2. Experimental

Similar to our previously reported experiments, the alloy ingots with nominal compositions of $\text{Fe}_{83.2}\text{P}_{10-x}\text{B}_x\text{C}_6\text{Cu}_{0.8}$ ($x = 0, 1, 2, 3, 4$ and 5 at.%) were prepared by induction melting the mixtures of pure raw materials of Fe (99.99 wt.%), Cu (99.995 wt.%), B (99.99 wt.%), pre-

* Corresponding authors.

E-mail addresses: ywmcumt666@163.com (W. Yang), blshen@seu.edu.cn (B. Shen).

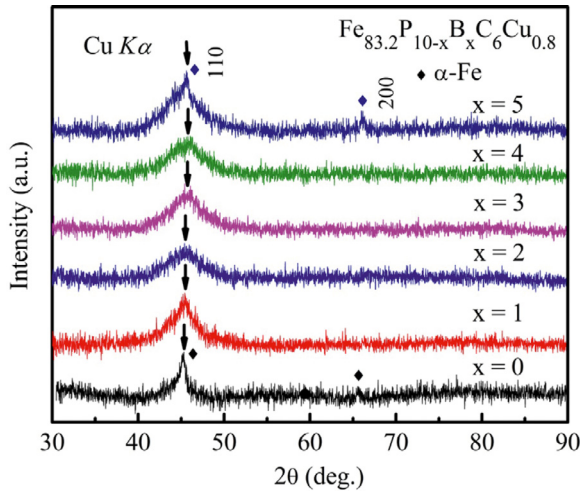


Fig. 1. XRD patterns of $\text{Fe}_{83.2}\text{P}_{10-x}\text{B}_x\text{Cu}_{0.8}$ ($x = 0, 1, 2, 3, 4$ and 5 at.%) AQ alloy ribbons.

alloyed Fe-P ingots (consisting of 75 wt.% Fe and 25 wt.% P) and Fe-C ingots (consisting of 96 wt.% Fe and 4 wt.% C) in an induction melting furnace under an argon atmosphere [18], and then the fragments of master alloy is prepared into the ribbons with about 26 μm thickness and 1 mm width by using the single roller melt-spinning method.

The microstructure was examined by X-ray diffraction (XRD, Bruker D8 Discover) with $\text{Cu K}\alpha$ radiation and transmission electron microscopy (TEM, FEI Tecnai G2 F20) and the detailed preparation of samples for TEM analyses seeing Ref. [18]. Thermal behaviors were measured using a differential scanning calorimeter (DSC, NETZSCH 404 F3) under a flow of high purity argon with a heating rate of $0.67\text{ }^\circ\text{C/s}$ [14]. The magnetic parameters including B_s , H_c and μ_e were measured with a vibrating sample magnetometer (VSM, Lake Shore 7410) under an applied field of 800 kA/m, a B-H loop tracer (RIKEN BHS-40) under a field of 1 kA/m and an impedance analyzer (Agilent 4294 A) under a field of 1 A/m at the room temperature, respectively.

3. Results and discussion

Fig. 1 displays the XRD patterns of free-side of $\text{Fe}_{83.2}\text{P}_{10-x}\text{B}_x\text{Cu}_{0.8}$ ($x = 0, 1, 2, 3, 4$ and 5 at.%) AQ ribbons. Small crystalline diffraction peaks around $2\theta = 45.2^\circ$ and 65.6° are observed for B-free alloy, which are related to the (110) and (200)-reflection of $\alpha\text{-Fe}$ crystalline phase [14,19], suggesting a poor AFA. As B content increases from 1 to 4 at.%, the small crystalline peaks obviously disappear, corresponding only broad diffuse diffraction peak for each alloy. This is the typical amorphous feature. With excessive B modification (5 at.%), the crystalline diffraction peaks occur again, indicating that proper B addition can improve the AFA of alloys effectively. Interestingly, it is found that the diffuse position of peak slightly shifts to a high side of 2θ , implying the variety of structural coordination and topological rearrangement of atoms by B addition. That is, the proper B content modification results in a denser packing structure with smaller interatomic distance and more coordination numbers, which is beneficial for the AFA [20].

Fig. 2 shows the DSC curves of $\text{Fe}_{83.2}\text{P}_{10-x}\text{B}_x\text{Cu}_{0.8}$ AQ alloys. For each curve, two distinct exothermic peaks can be observed, suggesting the alloy undergoes two different exothermic stages during the heating process. The first one corresponds to the precipitation of $\alpha\text{-Fe}$ and the second one is hard-magnetic Fe_3C compounds [10,14]. With B modification, the Curie temperature (T_c) of amorphous phase obviously increases, suggesting a difficult transition from the ferromagnetism to paramagnetism of amorphous matrix, which makes the studied ferromagnetic alloys used in a wide temperature range; the onset temperatures of the first and second crystallization peaks (T_{x1} and T_{x2}) all shift

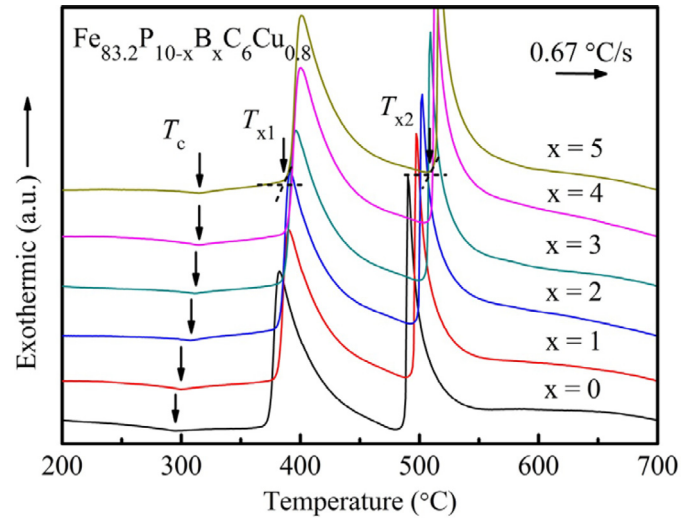


Fig. 2. DSC curves of $\text{Fe}_{83.2}\text{P}_{10-x}\text{B}_x\text{Cu}_{0.8}$ ($x = 0, 1, 2, 3, 4$ and 10 at.%) AQ alloy ribbons with a heating rate of $0.67\text{ }^\circ\text{C/s}$.

to a higher temperature level, indicating the high thermal stability of amorphous matrix. The temperature interval (ΔT_x) between T_{x1} and T_{x2} slightly increases from $114\text{ }^\circ\text{C}$ to $121\text{ }^\circ\text{C}$, meaning a larger crystallization window for heating treatment, which is better for optimizing the design of nanocrystalline alloy with good SMPs.

The magnetic performance of $\text{Fe}_{83.2}\text{P}_{10-x}\text{B}_x\text{Cu}_{0.8}$ AQ ribbons were measured with result shown in Fig. 3. The B_s of studied FePCCu AQ alloys with B addition is distinctly modified from 1.53 T to 1.64 T, which is larger than that of reported FePC [21], FePCB [17] and FeAlPBC [17] alloys, suggesting an effective modification on magnetic performance through the content adjusting of P and B. The molar volume (V_{mol}) which reflects the dense packing structure of Fe-based amorphous alloys was calculated via the density [22]. It can be seen that the variation of V_{mol} matches the opposite change of B_s well, suggesting a good connection between dense packing structure and magnetic performance. As we known, the magnetism is essentially determined by the magnetic moment, and the B_s reflects the amount of total magnetic moment for magnetic materials [23]. As the result of XRD, partial substitution of small size B for P inevitably leads to the reduction of atomic distance between magnetic Fe atoms in the FePBCCu system, which reinforces the bonding nature of Fe-Fe pairs that eventually leads to a higher atomic magnetic moment. Moreover, from electron configuration perspective, the p - d hybridization between magnetic metal and metalloid elements is a delocalization of some of the magnetic d states, and in consequence a large degradation of the effective magnetic moment of magnetic atoms [24]. With substitution of P by B, because B atom has one “ p ” electron compared to that of P atom having three, the annihilation of effective magnetic moment will be largely suppressed. All these results promote the high B_s of B-modified amorphous alloys. As also shown in Fig. 3, the H_c shows a trend of decreasing and then increasing, and reaches a lower value of 10.6 A/m with 2 at.% B addition. Previous work has given that the H_c can be roughly estimated by the following Eq. $H_c \approx \alpha(K/(\mu_0 M_s)) + \beta(\sqrt{(\lambda_s \sigma)/(\mu_0 M_s)})^2$, where the α , β is the constant, respectively, K is the magnetic anisotropy, μ_0 is the vacuum permeability, λ_s is the saturation magnetostriction, and σ represents the average absolute value of the residual stresses [25,26]. Thus, the variation in H_c may be attributed to the combined effect of saturation magnetization and residual stresses.

It is worth noting that the λ_s is another important factor affecting H_c , which will result in the magnetoelastic anisotropy. But the explanation of the magnetostrictive effects in such AQ alloys with precipitation of a small amount of $\alpha\text{-Fe}$ nanocrystals (B-free and 5 at.% B-

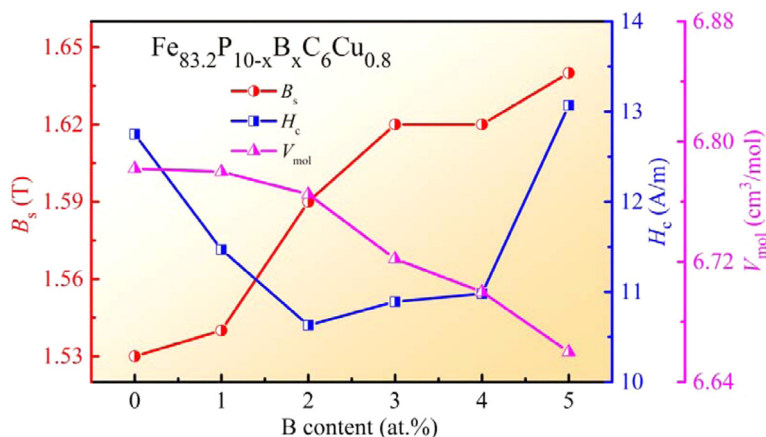


Fig. 3. The B_s , H_c and V_{mol} of $Fe_{83.2}P_{10-x}B_xC_6Cu_{0.8}$ ($x = 0, 1, 2, 3, 4$ and 5 at.%) AQ alloy ribbons with B addition.

modified alloy, respectively) is a difficult problem in which the properties of the respective phases, complex states of the internal stresses and strains as well as magneto-elastic interactions and the density of topological defects arising at the interfaces should be considered [27,28]. Also, the λ_s of the samples cannot be directly measured under our experimental conditions, but it can be one of the important directions for further study of SMPs in the future.

In order to obtain better performance Fe-based NAs and reveal their physical mechanism, the heat treatments of B-free and 2 at.% B-modified AQ ribbons were performed. The magnetic properties including B_s , H_c and μ_e are shown in Fig. 4. As given in Fig. 4(a), the B_s of both alloys gradually increases with annealing temperature (T_a). As T_a up to 450, 470 and 490 °C, the B-modified alloy achieves larger value of B_s of 1.77, 1.78 and 1.76 T, respectively. The increment of B_s may be related to the uniform refined nanocrystalline microstructure [14]. Clearly seeing from Fig. 4(b) that the H_c exhibits the obvious difference, especially, the H_c for B-modified alloy shows firstly decrease-increase and then

re-decrease-re-increase trend and the lowest value of 3.6 A/m compared to 8.2 A/m for B-free alloy at 450 °C is obtained, indicating that B modification can effectively ameliorate the SMPs of Fe-based NAs. Meanwhile, the μ_e shows the opposite trend compared to that of H_c as shown in Fig. 4(c). As a result, comprehensively excellent SMPs were obtained by annealing at 450 °C for 3 min, where the $Fe_{83.2}P_8B_2C_6Cu_{0.8}$ NA exhibits a high B_s of 1.77 T, low H_c of 3.6 A/m and high μ_e of 20,600.

Considering that the magnetic performance of Fe-based NAs are dependence on the microstructure and volume fraction (V_{cry}) of α -Fe nanocrystals in amorphous matrix, thus, the α -Fe phase after heat treatment for $Fe_{83.2}P_8B_2C_6Cu_{0.8}$ alloy was firstly identified using XRD as shown in Fig. 5. Noting that in the vicinity of T_{x2} (about 490 °C), the second compound of $Fe_3(C, B)$ is induced, which results in the deterioration of H_c of NAs, although the B_s is higher according to Fig. 4. Furthermore, HRTEM was also performed to reveal the underlying mechanism of microstructure and SMPs. Before and after heat treatment, the microstructure evolutions on SMPs for B-free and B-modified (2 at.%) alloys were elucidated. A small number of nanocrystals are embedded in B-free AQ amorphous matrix. The selected area electron diffraction (SAED) pattern also reveals the presence of nanocrystals [Fig. 6(a)], which is in agreement with the XRD result. Whereas, a typical amorphous feature for B-modified AQ alloy is identified, and the fast Fourier transformation (FFT) pattern only indicates some locally structural ordering/compositional fluctuations [Fig. 6(b)], which may

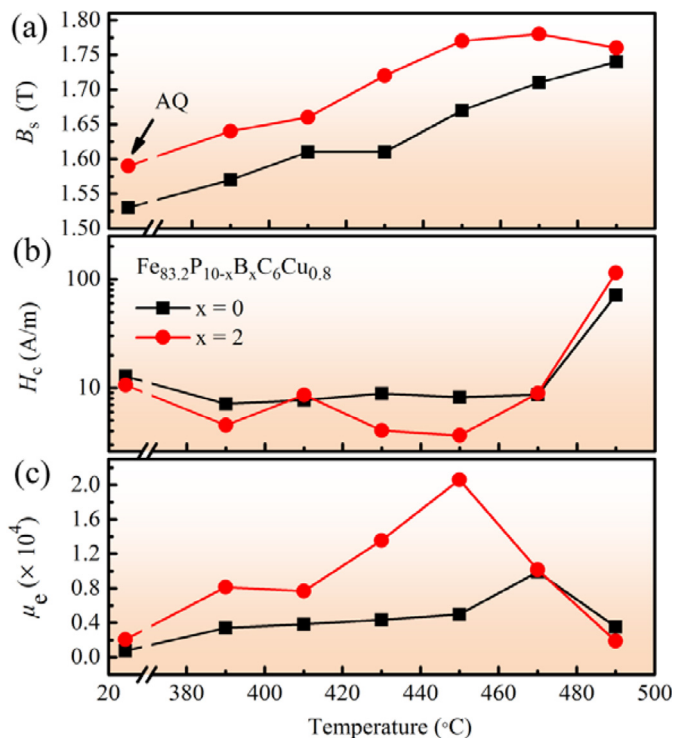


Fig. 4. The changes of B_s (a), H_c (b), and μ_e (c) with different annealing temperature for 3 min for $Fe_{83.2}P_{10-x}B_xC_6Cu_{0.8}$ ($x = 0$ and 2 at.%) alloy ribbons.

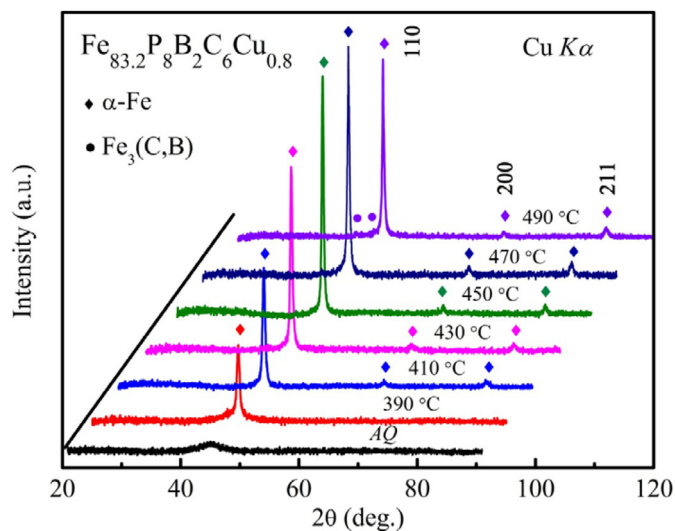


Fig. 5. XRD patterns of $Fe_{83.2}P_8B_2C_6Cu_{0.8}$ alloy after annealing at different temperatures.

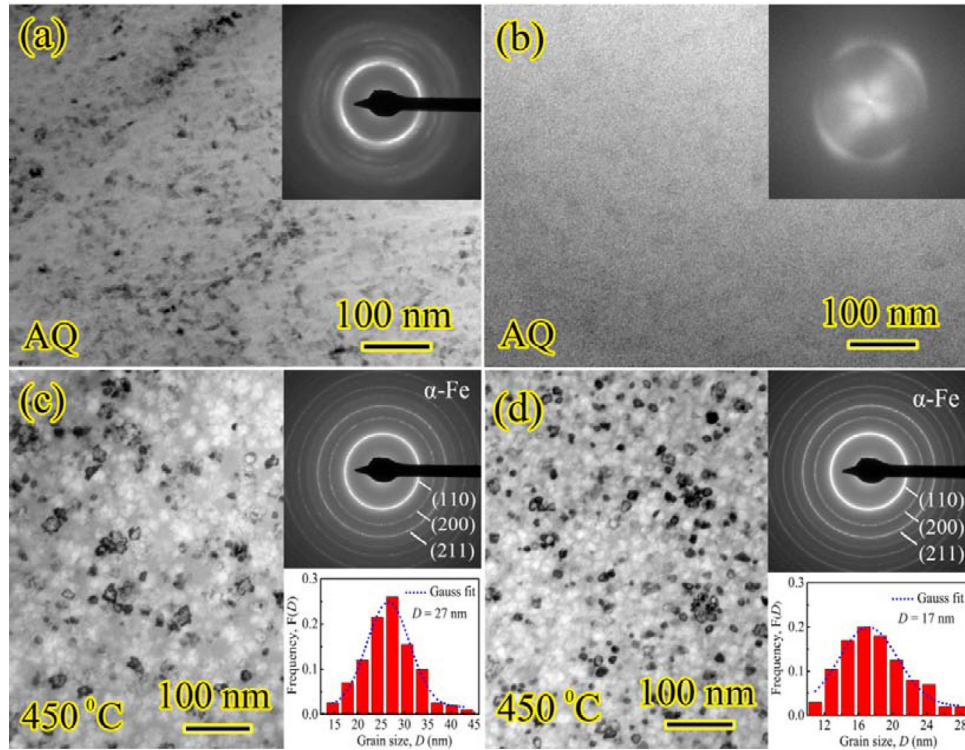


Fig. 6. The bright-field TEM images of $\text{Fe}_{83.2}\text{P}_{10-x}\text{B}_x\text{C}_6\text{Cu}_{0.8}$ alloys with (a) AQ: $x = 0$, the inset is the SAED pattern; (b) AQ: $x = 2$, the inset is the FFT pattern; (c) and (d) annealed: $x = 0$ and $x = 2$, the inset is the SAED pattern and grain size distribution, respectively.

Table 1

Magnetic properties and microstructure parameters of $\text{Fe}_{83.2}\text{P}_{10-x}\text{B}_x\text{C}_6\text{Cu}_{0.8}$, $\text{Fe}_{80}\text{P}_{11}\text{C}_9$, $\text{Fe}_{80}\text{P}_9\text{C}_9\text{B}_2$ and $\text{Fe}_{77}\text{Al}_3\text{P}_9\text{B}_2\text{C}_9$ nanocrystalline alloys. The B_s and V_{mol} of AQ alloys are also shown in the table for comparison.

Alloys	B_s -AQ T	V_{mol} cm^3/mol	Magnetic properties			Microstructure parameters		
			B_s T	H_c A/m	μ_c 1 kHz	D nm	V_{cry} %	N_d m^{-3}
$\text{Fe}_{83.2}\text{P}_{10}\text{C}_6\text{Cu}_{0.8}$	1.53	6.782	1.68	8.2	4980	27	30.9	3.1×10^{22}
$\text{Fe}_{83.2}\text{P}_9\text{B}_1\text{C}_6\text{Cu}_{0.8}$	1.54	6.780	1.72	5.3	16,980	24	42.3	6.3×10^{22}
$\text{Fe}_{83.2}\text{P}_8\text{B}_2\text{C}_6\text{Cu}_{0.8}$	1.59	6.765	1.77	3.6	20,630	17	47.0	1.8×10^{23}
$\text{Fe}_{83.2}\text{P}_7\text{B}_3\text{C}_6\text{Cu}_{0.8}$	1.62	6.722	1.69	6.0	13,950	23	20.3	3.3×10^{22}
$\text{Fe}_{83.2}\text{P}_6\text{B}_4\text{C}_6\text{Cu}_{0.8}$	1.62	6.700	1.69	6.4	10,300	23	19.1	3.1×10^{22}
$\text{Fe}_{83.2}\text{P}_5\text{B}_5\text{C}_6\text{Cu}_{0.8}$	1.64	6.660	1.68	8.4	6500	26	15.3	1.7×10^{22}
$\text{Fe}_{80}\text{P}_{11}\text{C}_9$ [21]	1.37	–	1.49	3.9	11,000	–	–	–
$\text{Fe}_{80}\text{P}_9\text{C}_9\text{B}_2$ [17]	1.46	–	1.56	–	–	78	–	–
$\text{Fe}_{77}\text{Al}_3\text{P}_9\text{B}_2\text{C}_9$ [17]	1.37	–	1.30	–	–	–	–	–
$\text{Fe}_{83.25}\text{P}_9\text{C}_7\text{Cu}_{0.75}$ [11]	–	–	1.64	3.9	21,000	23	–	–

be caused by Cu/CuP clusters [9,29]. After heat treatment (annealed at 450 °C for 3 min), the precipitated α -Fe nanocrystals are relatively large and non-uniform for B-free NA [Fig. 6(c)], which is related to the pre-existing α -Fe nanocrystals formed from the quenched liquid state. The statistic reveals the wide grain size (D) distribution of 15–45 nm with 27 nm in average and the corresponding number density (N_d) is $\sim 3.1 \times 10^{22} \text{ m}^{-3}$. On the contrary, high density and uniformity of α -Fe with small size of 17 nm in average can be observed for B-modified NA [Fig. 6(d)], and the N_d of $1.8 \times 10^{23} \text{ m}^{-3}$ is an order of magnitude larger than that of B-free alloy. Here, based on assuming spherical crystals from Fig. 6(c) and (d), the N_d of α -Fe nanocrystals can be calculated using the following Eq. $N_d = 6V_{\text{cry}} / (\pi D^3)$ [30]. So, the details can be seen in Table 1. These results imply that B modification can effectively inhibit the pre-existing α -Fe nanocrystals formed during quenched process, and the nucleation, growth and interaction of α -Fe adhering to locally structural ordering in amorphous matrix induces a more uniform refined nanocrystalline microstructure, which allows the strong exchange-coupling interaction between α -Fe nanocrystals and results in good SMPs.

Based on the discussion above, the relationship of magnetic performance dependence on microstructure is summarized in Fig. 7. One can see that H_c and D show almost the same correlation with B increasing, while B_s follows the varieties of V_{cry} and N_d . As a result, the 2 at.% B modified alloy exhibits the highest N_d with smallest D of grains, indicating the larger nucleation rate and slower growth rate of α -Fe nanocrystals. Whereas, for excessive B modified to alloy, although the D gradually grows, the N_d drops, and the latter is dominant, thus the reduction of V_{cry} leads to a decrement of B_s . The varieties of SMPs of Fe-based NAs are caused by the fact that magneto-crystalline anisotropy cannot be effectively averaged out due to the random distribution of the anisotropy axis of the nanograins [31]. The coercivity and permeability are expected to roughly vary with grain size as $H_c \propto D^6$ and $\mu_c \propto 1/D^6$, respectively [32]. Thus the deterioration of magnetic softness is due to the larger magneto-crystalline anisotropy induced by larger D and lower N_d of α -Fe nanocrystals. On the whole, with appropriate B addition (2 at.%) and annealing conditions, the $\text{Fe}_{83.2}\text{P}_8\text{B}_2\text{C}_6\text{Cu}_{0.8}$ nanocrystalline alloy with uniform refined microstructure exhibits the excellent soft-magnetic properties.

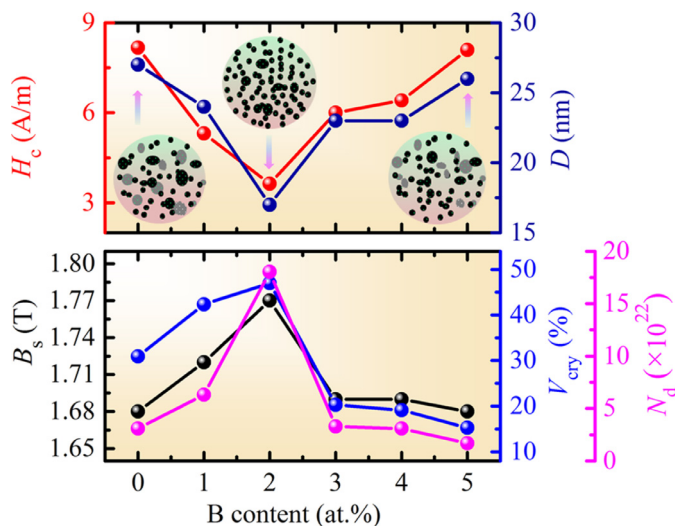


Fig. 7. Relationship of magnetic performance dependence on microstructure for FePBCu alloys.

4. Conclusion

In summary, we have identified that the B_s of FePBCu amorphous alloys can be essentially improved through the dense packing atomic structure induced by B substitution for P. Based on high B_s amorphous matrix, $\text{Fe}_{83.2}\text{P}_8\text{B}_2\text{C}_6\text{Cu}_{0.8}$ nanocrystalline alloy obtained by annealing at 450 °C for 3 min shows uniform microstructure with high V_{cry} of 47% and N_d of $1.8 \times 10^{23} \text{ m}^{-3}$ of α -Fe nanocrystals, and exhibits high B_s of 1.77 T, low H_c of 3.6 A/m and high μ_e of 20,600. The undulating changes in H_c and μ_e are closely associated with varieties of grain size D . The combination of high B_s and good SMPs promises the potential application of FePBCu nanocrystalline alloy in industrial magnetic devices.

Author contributions

Long Hou, Weiming Yang and Baolong Shen conceived and designed the research and analysis. Xingdu Fan and Qiang Luo analyzed the experimental data. Long Hou, Weiming Yang, Xingdu Fan and Haishun Liu co-wrote the paper. All authors discussed the results and revised the manuscript.

Declaration of Competing Interest

The authors declare that they have no known competing financial interests or personal relationships that could have appeared to influence the work reported in this paper.

Acknowledgments

This work was supported by the National Key Research and Development Program of China (grant no. 2016YFB0300502), the National Natural Science Foundation of China (grant no. 51631003 and 51871237) and the Fundamental Research Funds for the Central Universities (grant no. 2242019K40062).

References

- [1] Y. Yoshizawa, S. Oguma, K. Yamauchi, New Fe-based soft magnetic alloys composed of ultrafine grain structure, *J. Appl. Phys.* 64 (1988) 6044–6046.
- [2] M.E. McHenry, M.A. Willard, D.E. Laughlin, Amorphous and nanocrystalline materials for applications as soft magnets, *Prog. Mater. Sci.* 44 (1999) 291–433.

- [3] F.P. Wan, A.N. He, J.H. Zhang, J.C. Song, A.D. Wang, C.T. Chang, X.M. Wang, Development of FeSiBNbCu nanocrystalline soft magnetic alloys with high Bs and good manufacturability, *J. Electron. Mater.* 45 (2016) 4913–4918.
- [4] K. Suzuki, R. Parsons, B. Zang, K. Onodera, H. Kishimoto, A. Kato, Copper-free nanocrystalline soft magnetic materials with high saturation magnetization comparable to that of Si steel, *Appl. Phys. Lett.* 110 (2017) 012407.
- [5] J.G. Wang, H. Zhao, C.X. Xie, C.T. Chang, S.M. Zhou, J.Q. Feng, J.T. Huo, W.H. Li, In-situ synthesis of nanocrystalline soft magnetic Fe-Ni-Si-B alloy, *J. Alloys Compd.* 790 (2019) 524–528.
- [6] A. Makino, H. Men, T. Kubota, K. Yubuta, A. Inoue, Soft magnetic FeSiBPCu heteroamorphous alloys with high Fe content, *J. Appl. Phys.* 105 (2009) 07A308.
- [7] T. Liu, F.C. Li, A.D. Wang, X. Lei, Q.F. He, J.H. Luan, A.N. He, X.M. Wang, C.T. Liu, Y. Yang, High performance Fe-based nanocrystalline alloys with excellent thermal stability, *J. Alloys Compd.* 776 (2019) 606–613.
- [8] M. Ohta, Y. Yoshizawa, Magnetic properties of nanocrystalline $\text{Fe}_{82.65}\text{Cu}_{1.35}\text{Si}_x\text{B}_{16-x}$ alloys ($x = 0-7$), *Appl. Phys. Lett.* 91 (2007) 062517.
- [9] Y.M. Chen, T. Ohkubo, M. Ohta, Y. Yoshizawa, K. Hono, Three-dimensional atom probe study of Fe-B-based nanocrystalline soft magnetic materials, *Acta Mater.* 57 (2009) 4463–4472.
- [10] Y.L. Jin, X.D. Fan, M. He, X.C. Liu, B.L. Shen, FePCCu nanocrystalline alloys with excellent soft magnetic properties, *Sci. China Technol. Sci.* 55 (2012) 3419–3424.
- [11] R. Xiang, S.X. Zhou, B.S. Dong, G.Q. Zhang, Z.Z. Li, Y.G. Wang, The excellent soft magnetic properties and corrosion behaviour of nanocrystalline FePCCu alloys, *J. Mater. Sci. Mater. Electron* 25 (2014) 2979–2984.
- [12] A. Makino, T. Kubota, K. Yubuta, A. Inoue, A. Urata, H. Matsumoto, S. Yoshida, Low core losses and magnetic properties of $\text{Fe}_{85-86}\text{Si}_{1-2}\text{B}_3\text{P}_4\text{Cu}_1$ nanocrystalline alloys with high B for power applications (invited), *J. Appl. Phys.* 109 (2011) 07A302.
- [13] Z. Zhang, P. Sharma, A. Makino, Role of Si in high B_s and low core-loss $\text{Fe}_{85.2}\text{B}_{10.4}\text{P}_4\text{Cu}_{0.8}\text{Si}_x$ nano-crystalline alloys, *J. Appl. Phys.* 112 (2012) 103902.
- [14] L. Hou, X.D. Fan, Q.Q. Wang, W.M. Yang, B.L. Shen, Microstructure and soft-magnetic properties of FeCoPCCu nanocrystalline alloys, *J. Mater. Sci. Technol.* 35 (2019) 1655–1661.
- [15] L. Xue, W.M. Yang, H.S. Liu, H. Men, A.D. Wang, C.T. Chang, B.L. Shen, Effect of Co addition on the magnetic properties and microstructure of FeNBBCu nanocrystalline alloys, *J. Magn. Magn. Mater.* 419 (2016) 198–201.
- [16] A. Takeuchi, A. Inoue, Classification of bulk metallic glasses by atomic size difference, heat of mixing and period of constituent elements and its application to characterization of the main alloying element, *Mater. Trans.* 46 (2005) 2817–2829.
- [17] J.F. Wang, Y.X. Di, Z. Fang, S.K. Guan, T. Zhang, Thermal stability, crystallization and soft magnetic properties of Fe-P-C-based glassy alloys, *J. Non-Cryst. Solids* 454 (2016) 39–45.
- [18] L. Hou, Q.Q. Wang, X.D. Fan, F. Miao, W.M. Yang, B.L. Shen, Effect of Co addition on catalytic activity of FePCCu amorphous alloy for methylene blue degradation, *New J. Chem.* 43 (2019) 6126–6135.
- [19] X.D. Fan, T. Zhang, M.F. Jiang, W.M. Yang, B.L. Shen, Synthesis of novel FeSiBPCu alloys with high amorphous forming ability and good soft magnetic properties, *J. Non-Cryst. Solids* 503-504 (2019) 36–43.
- [20] Y.X. Geng, Y.M. Wang, J.B. Qiang, C. Dong, H.B. Wang, O. Tegus, Composition design and optimization of Fe-B-Si-Nb bulk amorphous alloys, *Acta Metall. Sin.* 52 (2016) 1459–1466.
- [21] J.F. Wang, R. Li, N.B. Hua, L. Huang, T. Zhang, Ternary Fe-P-C bulk metallic glass with good soft-magnetic and mechanical properties, *Scr. Mater.* 65 (2011) 536–539.
- [22] H.B. Ling, Q. Li, H.X. Li, J.J. Zhang, Y.Q. Dong, C.T. Chang, S. Yi, Preparation and characterization of quaternary magnetic $\text{Fe}_{80-x}\text{Co}_x\text{P}_4\text{B}_6$ bulk metallic glasses, *J. Appl. Phys.* 115 (2014) 204901.
- [23] Q.L. Liu, J.Y. Mo, H.S. Liu, L. Xue, L. Hou, W.M. Yang, L.T. Dou, B.L. Shen, L.M. Dou, Effects of Cu substitution for Nb on magnetic properties of Fe-based bulk metallic glasses, *J. Non-Cryst. Solids* 443 (2016) 108–111.
- [24] Z.M. Stadnik, G. Stroink, Electronic structure and magnetism of transition metal-metalloid glasses, *J. Non-Cryst. Solids* 99 (1988) 233–243.
- [25] P. Agudo, M. Vazquez, Influence of Ni on the structural and magnetic properties of $\text{Ni}_x\text{Fe}_{73.5-x}\text{Si}_{13.5}\text{B}_9\text{Nb}_3\text{Cu}_1$ ($0 \leq x \leq 25$) alloys, *J. Appl. Phys.* 97 (2005) 023901.
- [26] L.T. Dou, H.S. Liu, L. Hou, L. Xue, W.M. Yang, Y.C. Zhao, C.T. Chang, B.L. Shen, Effects of Cu substitution for Fe on the glass-forming ability and soft magnetic properties for Fe-based bulk metallic glasses, *J. Mag. Magn. Mater.* 358-359 (2014) 23–26.
- [27] A. Slawska-Waniewska, H.K. Lachowicz, Magnetostriction in soft magnetic nanocrystalline materials, *Scripta Mater.* 48 (2003) 889–894.
- [28] B.R. Sun, S.W. Xin, T.D. Shen, Microstructural origin of the ultra-low coercivity in bulk $\text{Fe}_{65.5}\text{Cr}_4\text{Mo}_4\text{Ga}_4\text{P}_{12}\text{B}_{5.5}\text{C}_5$ metallic glasses, *J. Mag. Magn. Mater.* 466 (2018) 130–132.
- [29] C.C. Cao, Y.G. Wang, L. Zhu, Y. Meng, X.B. Zhai, Y.D. Dai, J.K. Chen, F.M. Pan, Local structure, nucleation sites and crystallization behavior and their effects on magnetic properties of $\text{Fe}_{81}\text{Si}_x\text{B}_{10}\text{P}_{8-x}\text{Cu}_1$ ($x = 0-8$), *Sci. Rep.* 8 (2018) 1243–1254.
- [30] K.G. Pradeep, G. Herzer, P. Choi, D. Raabe, Atom probe tomography study of ultrahigh nanocrystallization rates in FeSiNBBCu soft magnetic amorphous alloys on rapid annealing, *Acta Mater.* 68 (2014) 295–309.
- [31] G. Herzer, Grain structure and magnetism of nanocrystalline ferromagnets, *IEEE Trans. Magn.* 25 (1989) 3327–3329.
- [32] R. Xiang, S.X. Zhou, B.S. Dong, Y.G. Wang, Effect of Nb addition on the magnetic properties and microstructure of FePCCu nanocrystalline alloy, *J. Mater. Sci.: Mater. Electron.* 26 (2015) 4091–4096.